CHAPTER 2

COMPUTATIONAL FRAMEWORK

In the field of gas sensing mechanisms, a profound understanding of the intricate interactions between gas molecules and two-dimensional material is paramount. These interactions form the bedrock upon which efficient gas sensors are built. While experimental procedures can yield valuable insights, they often demand substantial investments of time and finances. Computational approaches emerge as a potent and cost-effective avenue to delve into these molecular interactions at the atomic level. In this chapter, we delve into the computational methodologies essential to our gas sensing research. One of our primary tools is Quantum Espresso[1] employed for Density Functional Theory (DFT) calculations, a cornerstone in the study of molecular interactions.

This strategic junction not only opens the system's static attributes but also gives us access to its dynamic behaviour. It enables us to investigate time-dependent perturbation reactions and dig into the world of rheological properties, a multidimensional realm that includes electrical subtleties, structural dynamics, vibrational patterns, and crucial transfer parameters. This chapter provides a critical link to a thorough understanding of the molecular complexities that regulate gas interactions at the atomic scale, bringing us closer to the construction of highly efficient gas sensors.

2.1. Theory of Electronic Structure

2.1.1. Many body problem

A solid can be considered as an assembly of heavy nuclei and loosely bound electrons. In a solid with N nuclei, there are N + ZN electromagnetically interacting particles, where Z represents the atomic number. This system presents a many-body interaction problem. The ground state energies can be determined by solving the time-independent Schrödinger equation[2].

$$\hat{H}\psi = E\psi \text{ ---- } (2.1)$$

Here, Ψ represents the wave function for all particles, E is the energy eigenvalue of the system, and $\hat{H}$ is the many-particle Hamiltonian. The simplest example is the hydrogen atom, which consists of one electron and one proton. For this case, the Schrödinger equation can be solved exactly, yielding an energy of -13.6 eV for the hydrogen atom. However, in conventional solids, there are numerous electrons and ions, leading to complex interactions among them. Consequently, the Hamiltonian of the system becomes more complicated and is described by the following equation.

$$\hat{H} = \hat{T}_N + \hat{T}_e + \hat{V}_{ee} + \hat{V}_{eN} + \hat{V}_{NN} \quad \text{-----(2.2)}$$

were $\boldsymbol{\hat{T}_N}$ and $\boldsymbol{\hat{T}_e}$ are the kinetic energy operators for the nuclei and electrons respectively, $\boldsymbol{\hat{V}_{ee}}$, $\boldsymbol{\hat{V}_{eN}}$ and $\boldsymbol{\hat{V}_{NN}}$ are the potential energy due to the electron-electron interactions, electrons-nuclei interactions and nuclei-nuclei interactions respectively. The many body Schrödinger equation reads:

$$H\psi = [-\frac{\hbar^2}{2m_e}\sum_{i}\frac{\partial^2}{\partial\bar{r}_i{}^2} - \frac{\hbar^2}{2M}\sum_{l}\frac{\partial^2}{\partial\bar{R}_l{}^2} + \frac{1}{2}\sum_{\substack{l,l' \\ l\neq l'}}\frac{e^2}{4\pi\varepsilon_0}\frac{Z_l Z_{l'}}{|\bar{R}_l - \bar{R}_l{}'|}$$

$$+\frac{1}{2}\sum_{\substack{i,j \\ i\neq j}}\frac{e^2}{4\pi\varepsilon_0}\frac{1}{|\bar{r}_i - \bar{r}_j|} - \sum_i\sum_l\frac{e^2}{4\pi\varepsilon_0}\frac{Z_l}{|\bar{r}_i - \bar{R}_l|}]\psi = E\psi \quad \text{-----(2.3)}$$

where *i* and *l* are indices running for electron and nuclei, m_e and M stands for the mass of electron and nuclei, $\boldsymbol{Z_l}$ and $\boldsymbol{Z_{l'}}$ define the charges on different nuclei, $\boldsymbol{\bar{r}_i - \bar{r}_j}$, $\boldsymbol{\bar{R}_l - \bar{R}'_l}$ and $\boldsymbol{\bar{r}_i - \bar{R}_l}$ represent distances between electron-electron, nuclei-nuclei and electron-nuclei respectively. The solution of the equation (2.1) is the eigen state and energy eigen value which is the total energy of the system from which the ground state properties of materials at equilibrium condition can be obtained. The Hamiltonian in equation 2.3 involves atomic mass and charge of electron, atomic number and mass of nuclei, therefore the solution of equation 2.1 does not require any adjustable parameter owing to which the method is known as first-principles calculation. In practice, for smaller system such as hydrogen the equation 2.1 is easily solvable, but is difficult to solve for large systems and for that several approximations were proposed.

2.2. Wave function-based methods to solve many body problem

2.2.1. The Born-Oppenheimer approximation

Nuclei are heavier and move more slowly compared to electrons. Born and Oppenheimer assumed that nuclei can be considered static relative to the moving electrons, allowing the kinetic energy of the nuclei to be neglected[3]. As a result, the wave function can be divided into two parts: the electronic part and the ionic part, leading to a many-body wave function.

$$\psi = \chi_l(\bar{R})\ \phi_i(\bar{r},\ \bar{R}) \quad \text{------(2.4)}$$

Here $\chi_I(\bar{R})$ represents ionic, while $\phi_i(\bar{r},\, \bar{R})$ stands for electronic wave function. Following equations are separated ionic and electronic parts of wave function:

$$\left[-\frac{\hbar^2}{2M}\sum_I \frac{\partial^2}{\partial \bar{R_I}^2} + V_{NN}(\bar{R}) + E_E(\bar{R})\right]\chi_I(\vec{R}) = E\chi_I(\bar{R}) \text{ -----(2.5)}$$

$$\left[-\frac{\hbar^2}{2m_e}\sum_i \frac{\partial^2}{\partial \bar{r_i}^2} + V_{Ne}(\bar{r},\, \bar{R}) + V_{ee}(\bar{r})\right] \phi_i(\bar{r},\, \bar{R}) = E_e\, \phi_i(\bar{r},\, \bar{R}) \text{------(2.6)}$$

Here, in the above two equations derived from equation 2.2, where the first term of equation 2.2 vanishes under Born-Oppenheimer (BO) approximation and the last term will be a constant[4].The residual Hamiltonian will now be read as:

$$\hat{\boldsymbol{H}} = \hat{\boldsymbol{T}}_{\boldsymbol{e}} + \hat{\boldsymbol{V}}_{\boldsymbol{ee}} + \hat{\boldsymbol{V}}_{\boldsymbol{eN}} + \text{ Constant ------ (2.7)}$$

The Hamiltonian operator ($\hat{H}$) can be modified as a sum of kinetic energy of electrons, the electron-electron interaction ($\hat{V}_{ee}$) and the interaction with the external potential ($\hat{V}_{ext}$):

$$\hat{H} = \hat{T}_e + \hat{V}_{ee} + \hat{V}_{ext} \quad \text{------ (2.8)}$$

where the electron kinetic energy operator $\hat{T}_e$ for the electrons is:

$$\hat{T}_e = \frac{-\hbar^2}{2m_e}\sum_i \frac{\partial^2}{\partial \bar{r_i}^2} \quad \text{------ (2.9)}$$

and the potential energy $\hat{V}_{ee}$ due to electron-electron interactions is:

$$\hat{V}_{ee} = \frac{1}{2}\sum_{i\neq j} \frac{e^2}{|r_i - r_j|} \quad \text{------- (2.10)}$$

The external potential of interest is the electron-nuclei interaction and is given by

$$\hat{V}_{ext} = \sum_{i,I} V_I(|r_i - R_I|) \text{ ------- (2.11)}$$

were r_i is the coordinate of ith electron and $\hat{V}_{ext}$ is the external potential.

2.2.2. Hartree approximation

In the Hartree approximation, electron-electron interaction is based on classical electrostatics, where Coulomb repulsion is considered in some form. In classical electrostatics, an electronic charge distribution n(r) generates an electrostatic potential through Poisson's equation[5].

$$\nabla^2 \varphi(r) = 4\pi n(r) \text{ --------(2.12)}$$

Electrons subjected to this potential will have a potential energy known as the Hartree potential, which satisfies Poisson's equation[5].

$$\nabla^2 V_H(r) = -4\pi n(r) \text{ --------(2.13)}$$

The solution of equation 2.9 in Hartree units, will have the form: a potential energy $V_H(r) = -\varphi(r)$, which is called the Hartree potential

$$E_H[n] = \frac{1}{2}\frac{n(r)n(r')}{|r-r'|} d^3r d^3r' \text{ --------(2.14)}$$

With the inclusion of Hartree potential one can write the complete Schrödinger's equation for electronic part as follows:

$$-\frac{\hbar^2}{2m_e}\nabla_i{}^2\phi_i - \frac{1}{4\pi\varepsilon_0}\sum_l \frac{Ze^2}{|\bar{r}_i-\bar{R}_l|}\phi_i + \frac{1}{4\pi\varepsilon_0}\sum_{j\neq i}\int \frac{e^2|\Psi_j|^2}{|\bar{r}_i-\bar{r}_j|} d^3r_j = \epsilon_i\ \phi_i \text{ ----(2.15)}$$

The first term on the left-hand side of the equation represents the kinetic energy of the electrons, the second term denotes the ion-electron interaction (V_{IE}) that depends solely on the electron's position, and the final term represents the Hartree potential (V_H). This equation, equation (2.11) known as the Hartree equation, is solved using the variational principle, which yields the ground state energy by minimizing the expectation value of energy E.

$$E = \frac{\langle \Psi_H | H | \Psi_H \rangle}{\langle \Psi_H | \Psi_H \rangle} \text{ ------ (2.16)}$$

Hartree transformed the many-body problem into a single-electron problem, known as the independent electron approximation. This approach neglects electron correlations and the asymmetric nature of the electron wave function.

2.2.3. Hartree-Fock (HF) approximation

As fermions, electrons follow Pauli's exclusion principle, so their wave function's asymmetric nature and the effects of electron correlation cannot be ignored. Hartree and Fock took into account the asymmetric wave function, described by the following equation[6]:

$$\Psi_{HF}(\overline{r_1}, \sigma_1, \dots, \overline{r_i}, \sigma_i, \ \dots, \overline{r_j}, \sigma_j, \dots) = -\Psi_{HF}(\overline{r_1}, \sigma_1, \dots, \overline{r_i}, \sigma_i, \ \dots, \overline{r_j}, \sigma_j, \dots) \text{ ----- (2.17)}$$

In HF approximation, minimization of equation 2.15 is done by considering the above asymmetric wave function in the determinant form known as **Slater's determinant**[7].

$$\Psi_{HF}(\overline{r_1},\sigma_1,\dots,\overline{r_N},\sigma_N)=\begin{vmatrix}\Psi_1(\overline{r_1},\sigma_1) & \Psi_1(\overline{r_2},\sigma_2)\dots & \Psi_1(\overline{r_N},\sigma_N)\\ \Psi_2(\overline{r_2},\sigma_2) & \Psi_2(\overline{r_2},\sigma_2)\dots & \Psi_2(\overline{r_N},\sigma_N)\\ \Psi_N(\overline{r_N},\sigma_N) & \Psi_N(\overline{r_N},\sigma_N)\dots & \Psi_N(\overline{r_N},\sigma_N)\end{vmatrix} \text{ ----- (2.18)}$$

The determinant of the wave function can be written as

$$\Psi_{HF}=\frac{1}{N!}\sum_P(-1)^p P\,\Psi_1(x_1)\,\Psi_2(x_2)\dots\,\Psi_N(x_N) \text{ ----- (2.19)}$$

where, $x=(\bar{r},\sigma)$, P is the permutation number and p is number of interchanges for making up this permutation. Substituting the Slater determinant of many body wave function in equation 2.15 gives expectation value of Hamiltonian as

$$E=\sum_i\int\Psi^*(\vec{r})\left[-\frac{\hbar^2}{2m_e}\sum_i\nabla_i^2+V_l(\vec{r})\right]\Psi(\vec{r})d^3r\,\frac{1}{2}\sum_i\sum_{i\neq j}\iint\frac{e^2}{4\pi\varepsilon_0}\frac{|\Psi_i(x_i)||\Psi_j(x_j)|^2}{|\vec{r}-\vec{r}'|}d^3rd^3r'$$

$$-\frac{1}{2}\sum_{i,j}\sum_{j\neq i}\iint\frac{e^2}{4\pi\varepsilon_0}\frac{\Psi_i^*(\vec{r})\Psi_j^*(\vec{r}')\,\Psi_i(\vec{r}')\,\Psi_j(\vec{r})}{|\vec{r}-\vec{r}'|}d^3rd^3r' \text{ ----- (2.20)}$$

where the last term is the consequence of Pauli's exclusion principle known as exchange energy. Minimization of equation 2.17 leads to Hartree-Fock equation:

$$\left[-\frac{\hbar^2}{2m_e}\sum_i\nabla^2-V_l(\vec{r})+V_H(\vec{r})\right]\Psi_i(\vec{r})-\frac{1}{2}\sum_{i,j}\sum_{j\neq i}\iint\frac{e^2}{4\pi\varepsilon_0}\frac{\Psi_j^*(\vec{r}')\,\Psi_i(\vec{r}')\,\Psi_j(\vec{r})}{|\vec{r}-\vec{r}'|}d^3rd^3r'$$

$$=\ \in_i\Psi_i(\vec{r}) \text{ ----- (2.21)}$$

This method improves upon the Hartree approach by incorporating exchange energy and considering the asymmetric nature of the wave function. However, the total energy $\in_i$ requires minimization over the sum of N-particle Slater determinants (equation 2.15). Such determinants are quite large, making this approximation computationally expensive for both large and small systems.

2.3. Density based method: Density functional theory

The ultimate goal is to determine the ground state energy of a many-electron system by solving the many-body Schrödinger equation (equation 2.3). For a system with N electrons, there are 3N variables, making the solution of equation 2.3 complex. Density functional theory (DFT) uses a density-based method where the interaction energy and potentials depend only on the electron density, significantly reducing the computational cost.

2.3.1. Thomas-Fermi theory

The initial method for solving many-body systems to compute the ground state energy using density-based theory was developed from the Thomas-Fermi (TF) theory[8,9]. In 1927, Thomas and Fermi suggested that the electron density could serve as a fundamental variable instead of single-particle wave functions or orbitals. They proposed that the total energy of the system could be expressed as a functional of the electron density. The kinetic energy of N interacting electrons can be written in terms of the electron density $n(\bar{r})$ as follows**:**

$$T_{TF} = C_k \int n(\bar{r})^{\frac{5}{3}} d^3r \text{ ----- (2.22)}$$

The total energy can be written as a functional of electron density by adding the kinetic energy, electrostatic energy and external potential as a functional of electron density

$$E = T_{TF} + \int V_{IE}(\bar{r})\, n(\bar{r}) d^3r + \frac{1}{2} \iint \frac{e^2}{4\pi\varepsilon_0} \frac{n(\vec{r}')\, n(\vec{r})}{|\vec{r}-\vec{r}'|} d^3r d^3r' \text{ ---- (2.23)}$$

where E is the Total energy. The total number of particles can be obtained by the minimization of above energy with constraint recognized by Lagrange multiplier as:

$$\frac{5}{3} C_k n(\bar{r})^{\frac{2}{3}} + \int \frac{e^2}{4\pi\varepsilon_0} \frac{n(\vec{r}')}{|\vec{r}-\vec{r}'|} d^3r' = \mu \;\; ; \mu = \frac{5}{3} C_k n(\bar{r})^{\frac{2}{3}} + V(\bar{r}) \text{ ------ (2.24)}$$

Equation 2.23 can be solved iteratively. In Thomas-Fermi theory, the exchange energy is not included. Dirac expanded upon this method to incorporate exchange interaction and correlation functionals[10]. However, Thomas-Fermi theory does not account for the shell structure and atomic behaviours of complex systems.

2.3.2 Hohenberg and Kohn theorem

In 1964, Hohenberg and Kohn established two fundamental theorems that underpin density functional theory calculations[11,12]. The schematic of these theorems is illustrated in Figure 2.1. The first theorem, Theorem I, states:

"For any system of interacting particles in an external potential $V_{ext}(\mathbf{r})$, this potential is uniquely determined, up to a constant, by the ground state particle density n(r)"

According to Theorem I, the ground state of a system uniquely depends on its density. Therefore, given the charge density, the Hamiltonian operator can be uniquely determined, allowing for the computation of the wave function *Ψ* and all material properties. The proof of Theorem 1 is presented below:

Consider two different external potentials $V_{ext}^{(1)}(r)$ and $V_{ext}^{(2)}(r)$ differing by more than a constant and leading to different ground state wave functions, $\Psi^{(1)}$ and $\Psi^{(2)}$ respectively. Let us assume same ground state density n(r) for both potentials. The two external potentials lead to two different Hamiltonians, $\hat{H}^{(1)}$ and $\hat{H}^{(2)}$. Since $\Psi^{(2)}$ is not the ground state of $\hat{H}^{(1)}$.

$$E^{(1)} = \langle \Psi^{(1)} | \hat{H}^{(1)} | \Psi^{(1)} \rangle < \langle \Psi^{(2)} | \hat{H}^{(1)} | \Psi^{(2)} \rangle \text{ -----(2.25)}$$

The last term can be rewritten as:

$$\langle \Psi^{(2)} | \hat{H}^{(1)} | \Psi^{(2)} \rangle = \langle \Psi^{(2)} | \hat{H}^{(2)} | \Psi^{(2)} \rangle + \langle \Psi^{(2)} | \hat{H}^{(1)} - \hat{H}^{(2)} | \Psi^{(2)} \rangle \text{ ----- (2.26)}$$

$$= E^{(2)} + \int \left[V_{ext}^{(1)}(r) - V_{ext}^{(2)}(r) \right] n(r) d^3 r \text{ ----- (2.27)}$$

so that

$$E^{(1)} < E^{(2)} + \int \left[V_{ext}^{(1)}(r) - V_{ext}^{(2)}(r) \right] n(r) d^3 r \text{ ----- (2.28)}$$

It is reasonable to interchange the labels 1 and 2.

$$E^{(2)} < E^{(1)} + \int \left[V_{ext}^{(1)}(r) - V_{ext}^{(2)}(r) \right] n(r) d^3 r \text{ ----- (2.29)}$$

Adding equations (2.25) and (2.26) gives

$$E^{(1)} + E^{(2)} < E^{(2)} + E^{(1)} \text{ ----- (2.30)}$$

Which contradicts our assumption and proves that there can only be one external potential $V_{ext}(r)$ that produces the ground state density $n(r)$, and conversely that the external potential $V_{ext}(r)$ is uniquely determined by the ground state density.

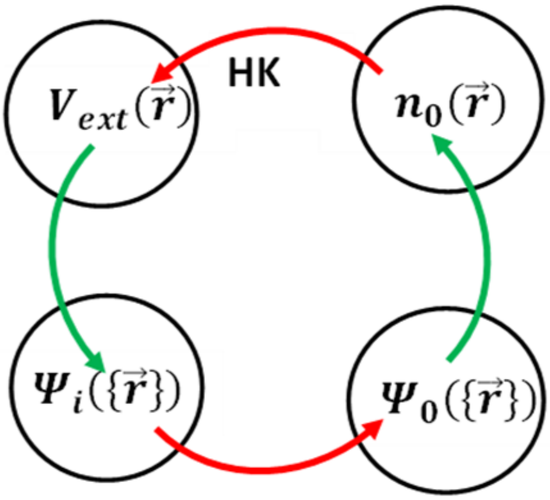

Figure 2.1: *Schematic representation of first Hohenberg and Kohn theorem. Here, the HK theorem completes the circle, while arrow shows the solution of Schrödinger equation.*

The second theorem is stated as follows;

Theorem II: *"The functional that delivers the ground state energy of the system, describes the lowest energy if and only if the input density is the true ground state density."*

We can now examine a system where the ground state density $n^{(1)}(r)$ corresponds to the external potential $V_{ext}^{(1)}(r)$. The universal functional can be written as:

$$E[n] = F[n] + \int V_{ext}(r) n(r) d^3r \text{ ---- (2.31)}$$

$$\text{where } F[n] = T[n] + E[n]_{int} \text{ ---- (2.32)}$$

Therefore a different density, $n^{(2)}(r)$ corresponds to a different wave function $\Psi^{(2)}$, implying that the $E^{(2)}$ of this state is greater than $E^{(1)}$, since

$$E^{(1)} = \left\langle \Psi^{(1)} \middle| \hat{H}^{(1)} \middle| \Psi^{(1)} \right\rangle < \left\langle \Psi^{(2)} \middle| \hat{H}^{(1)} \middle| \Psi^{(2)} \right\rangle = E^{(2)} \text{ ---- (2.34)}$$

The energy calculated using equation (2.31) for the correct ground state density $n_0(r)$ is lower than the energy obtained using any other density $n(r)$. This principle is known as the second Hohenberg-Kohn theorem. The universal functional F[n] achieves the minimum energy only when the input density is the true ground-state density n_0.

2.3.3. The Kohn-Sham equation

The Hohenberg-Kohn theorems allow the energy to be divided into two parts: a system-dependent part $\int V_{ext}(r) n(r) d^3r$ and an unknown functional $F[n]$ as shown in equation 2.28. Kohn and Sham proposed a form for the unknown $F[n]$. They transformed density functional theory (DFT) into a practical tool by constructing an auxiliary system of non-interacting quasiparticles that have the same density as the true interacting system[12]. By developing good approximations for these functionals, direct minimization of the energy becomes possible. According to the Hohenberg-Kohn theorem, if a system of non-interacting electrons exists with the same density as the interacting system, the total energy of the interacting system can be expressed as follows.

$$E[n] = T[n] + V[n] + \int V_{ext}(r) n(r) d^3r \quad \text{------------ (2.35)}$$

where T[n], V[n] and $V_{ext}(r)$ are the kinetic energy functional, Coulomb potential functional and external potential respectively.

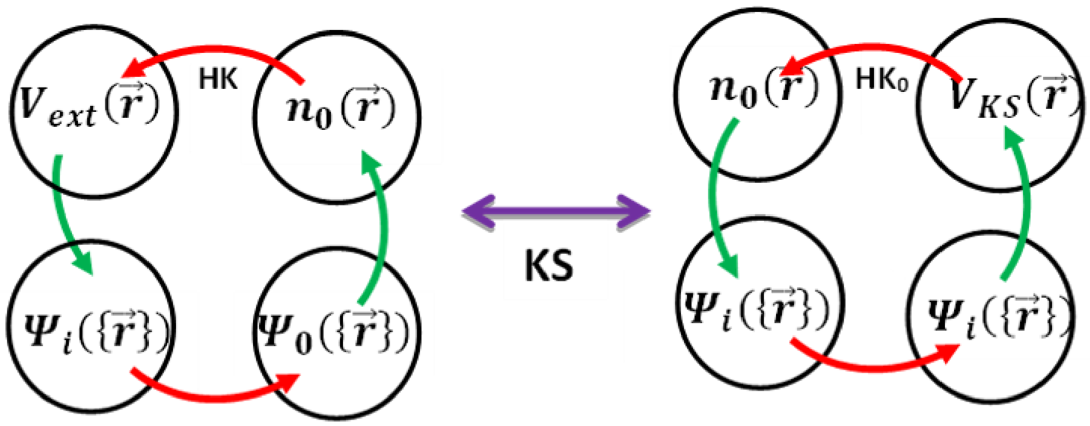

Figure 2.2: The connection between many body and the independent particle system is provided by Kohn – Sham, where HK_0 defines Hohenberg and Kohn theorem applied to non-interacting system

Since the single particle system and the interacting system are assumed to have the same density, adding and subtracting $T_s[n]$ (the non-interacting kinetic energy) and $E_H[n]$ (the Hartree energy) to (2.24), gives[13]

$$E_{KS}[n]=T_s[n]+E_H[n]+\{T[n]-T_s[n]+V[n]-E_H[n]\}+\int V_{ext}(r)n(r)d^3r \quad \text{---- (2.36)}$$

$$E_{KS}[n]=T_s[n]+E_H[n]+E_{xc}[n]+\int V_{ext}(r)n(r)d^3r \quad \text{---- (2.37)}$$

where the exchange-correlation energy is defined as:

$$E_{xc}[n]=T[n]-T_s[n]+V[n]-E_H[n] \quad \text{---- (2.38)}$$

In this context, the difference in kinetic energy $T[n]-T_s[n]$ represents the kinetic contribution to correlation, while the difference $V[n]-E_H[n]$ accounts for the electrostatic and Hartree-Fock exchange contributions to correlation. Although the exchange-correlation potential encompasses all significant quantum many-body effects, determining the exact exchange-correlation functional is highly challenging. Therefore, approximations are made using simple functionals, as discussed in Section 2.5.

The Hartree energy $E_H[n]$ in equation 2.27 is the classical electrostatic energy for a charge distribution *n(r)* given by equation 2.10. The non-interacting kinetic energy T_s, *density n(r)* and particle count N of the non-interacting system can be evaluated from the single particle wave functions as:

$$T_s[n]=-\frac{1}{2}\sum_i^N\langle\psi_i|\nabla^2|\psi_i\rangle \quad \text{--- (2.39)}$$

$$n(r) = \sum_{i}^{N} |\psi_i(r)|^2 \text{ ---- (2.40)}$$

$$N = \int n(r) d^3 r \text{ ---- (2.41)}$$

Ts[n] is explicitly expressed as a functional of the orbital's whereas all other terms are functionals of the density, then solution of equation 2.39 is the problem of minimization with respect to density *n(r)*.

$$\frac{\delta E_{KS}}{\delta \psi_i^*(r)} = \frac{\delta T_s[n]}{\delta \psi_i^*(r)} + \left[\frac{\delta E_{ext}[n]}{\delta n(r)} + \frac{\delta E_H[n]}{\delta n(r)} + \frac{\delta E_{xc}[n]}{\delta n(r)} \right] \frac{\delta n(r)}{\delta \Psi_i^*(r)} = 0 \text{ ---- (2.42)}$$

From equation (2.35) and (2.37):

$$\frac{\delta T_s[n]}{\delta \psi_i^*(r)} = -\frac{1}{2} \nabla^2 \psi_i(r) \quad \text{and} \quad \frac{\delta n(r)}{\delta \psi_i^*(r)} = \psi_i(r) \text{ ---- (2.43)}$$

which leads to the Schrödinger like equations:

$$(H_{KS} - \varepsilon_i)\psi_i(r) = 0 \text{ ---- (2.44)}$$

where the ε_i are the eigen values, and H_{KS} is the effective Hamiltonian

$$H_{KS}(r) = -\frac{1}{2}\nabla^2 + V_{KS}(r) \text{ ---- (2.45)}$$

$$V_{KS}[r] = V_{ext}[r] + V_H[r] + V_{xc}[r] \text{ ---- (2.46)}$$

Equations (2.44) to (2.46), known as the Kohn-Sham equations, define the total energy E_{KS} and density n(r) as provided in equations (2.36) and (2.40). These equations describe independent particle systems, where the potential is determined self-consistently from the density. If the exact functional $E_{xc}[n]$ is known, the precise ground state density and energy can be obtained.

2.3.4. Self-consistent loop

The previous section provides an in-depth explanation of Kohn-Sham (KS) theory and the derivation of the KS equation. In practice, solving the KS equation involves numerically adjusting the electron density and effective potential iteratively to achieve self-consistency. Figure 2.3 illustrates the self-consistent process for solving the KS equation in a schematic manner. To solve the KS equation, the effective potential must be determined. Both the Hartree potential and the exchange-correlation potential are dependent on the electron density, which determines the correlation energy. An initial guess for the electron density is typically made by summing the densities of isolated atoms arranged as they are in the material.

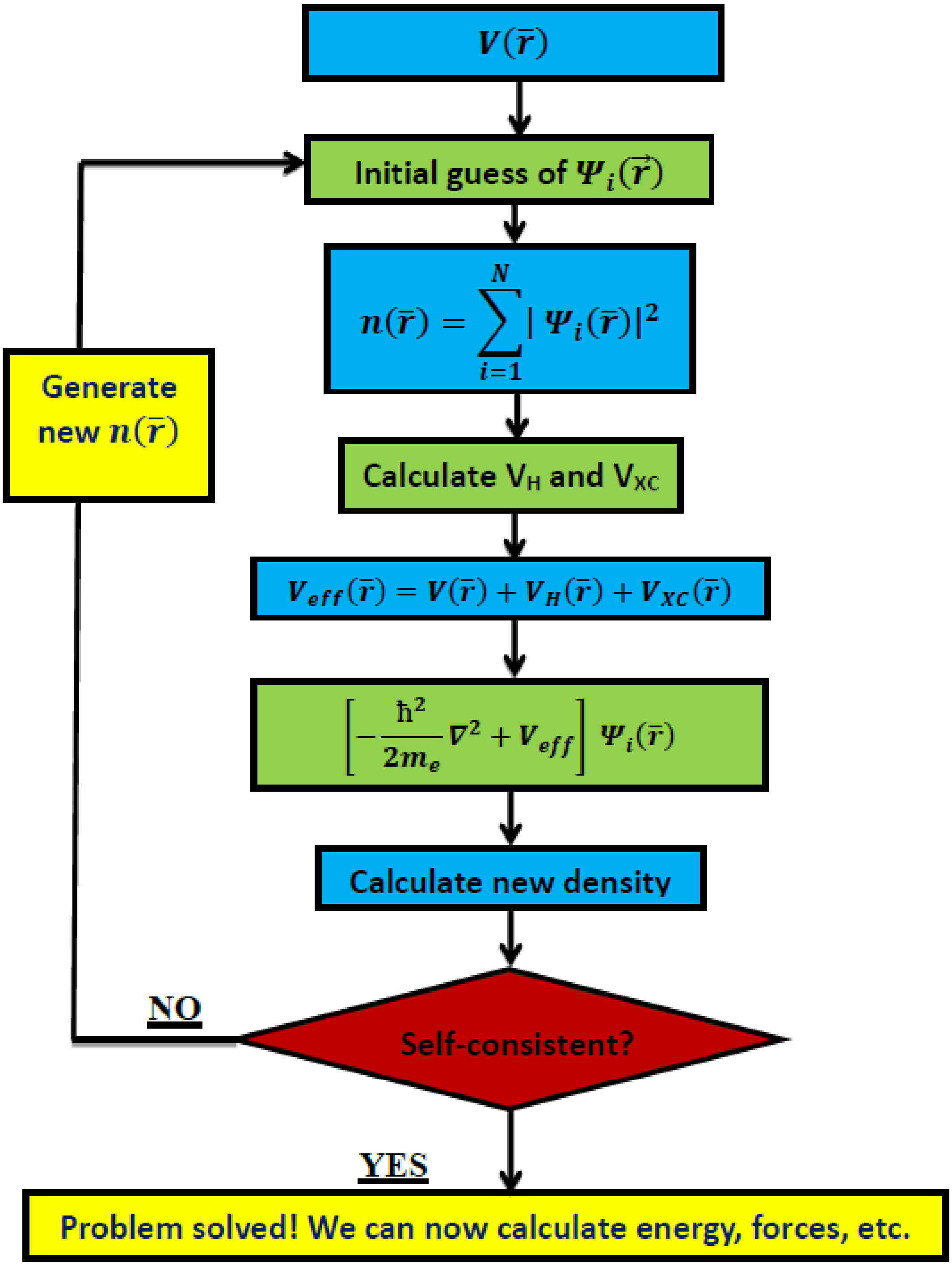

Figure 2.3: *Schematic flowchart to find the solution of KS equation.*

The computational solution of the KS equation involves several key steps. First, an initial guess for the electron density is made, often by specifying the nuclear coordinates, which provide *V(r)* and the exchange potential. The effective potential is then calculated, and a new density is derived from the unknown wave function obtained by solving the KS equations. If the new density matches the old density within a predefined tolerance, self-consistency is achieved; otherwise, the process iterates with a new effective potential derived from the updated electron density. This iterative process is computationally intensive, requiring efficient numerical methods and algorithms. Techniques such as density mixing, convergence acceleration schemes, and sophisticated diagonalization methods are often employed to enhance the stability and speed of convergence. Additionally, parallel computing and advanced computational resources are typically utilized to handle the large-scale matrix operations and integrations involved in the KS loop. Once the ground state density is obtained, the total energy of the system is calculated using the equation[14]:

$$E[n] = 2\sum_{\upsilon=1}^{N} \epsilon_{\upsilon} - \frac{e^2}{2}\int d\boldsymbol{r}d\boldsymbol{r}' \frac{n(\boldsymbol{r})n(\boldsymbol{r}')}{|\boldsymbol{r}-\boldsymbol{r}'|} + E_{xc}[n] - \int d\boldsymbol{r}n(\boldsymbol{r})V_{xc}(\boldsymbol{r}) + E_{Ewald} \quad \text{------(2.47)}$$

In this equation, E_{Ewald} represents the nuclear-nuclear interaction energy, which is calculated using the Ewald summation method[15].

2.4 Exchange and correlation functionals

Developing approximations for the exchange-correlation energy (E_{XC}) has been a significant focus of research in density functional theory. Various functionals have been created for specific scenarios and validated by comparing their results with experimental data. The most commonly used approximations are the local density approximation (LDA) and the generalized gradient approximation (GGA). The exchange-correlation functionals are computed as:

$$\boldsymbol{E_{xc} = \int n(r)\, V_x(r) F_{xc}(\ldots\ldots) d^3r} \quad \text{---- (2.48)}$$

where F_{xc} is the enhancement factor, with parameters that vary depending on whether the functional is LDA, GGA, or another high-level functional.

2.4.1. Local density approximation (LDA)

In the local density approximation (LDA), the functional is assumed to depend on the electron density of a homogeneous electron gas (HEG)[16]. This is the most commonly used approximation for exchange-correlation energy[17]. It is assumed that each infinitesimal volume element of a system has the same exchange-correlation energy as a homogeneous electron gas at the same density. The exchange and correlation energy in LDA is expressed as:

$$E_{xc}^{LDA}[n] = \int^{\int^{3}} n(r)\varepsilon_{xc}^{hom(n)} \quad \text{---- (2.49)}$$

Taking spin into account one can have spin polarized generalization of the approximation (LSDA) which is given as:

$$E_{xc}^{LSDA}[n^{\uparrow}, n^{\downarrow}] = \int^{\int^{3}} n(r)\varepsilon_{xc}^{hom}\left(n^{\uparrow}, n^{\downarrow}\right) \quad \text{---- (2.50)}$$

$$E_{xc}^{LSDA}\left[n^{\uparrow},n^{\downarrow}\right]=\int n(r)\left[\varepsilon_{x}^{\text{hom}}\left(n^{\uparrow},n^{\downarrow}\right)+\varepsilon_{c}^{\text{hom}}\left(n^{\uparrow},n^{\downarrow}\right)\right]d^{3}r \text{ ---- (2.51)}$$

The homogeneous electron gas (HEG) is a system similar to an ideal metal in a neutral state, where electrons move in a background of positive charge distribution. The electron density $n = N/\Omega$ is assumed to be constant throughout. The LDA provides accurate geometrical parameters and bulk moduli, and phonon frequencies are accurate to within a few percent. However, in realistic systems, where the density varies rapidly, the LDA does not produce accurate physical properties. The form of the exchange-correlation energy functionals is known exactly, or at least with very high accuracy, for the homogeneous electron gas model.

The exchange-correlation (XC) functional is the sum of a correlation functional and an exchange functional:

$$\varepsilon_{xc}^{\text{hom}}(n)=\varepsilon_{x}^{\text{hom}}(n)+\varepsilon_{c}^{\text{hom}}(n) \text{ ---- (2.52)}$$

The per electron exchange energy for homogeneous system is:

$$\varepsilon_{x}^{\text{hom}}(n)=-\frac{3}{4}\left(\frac{3}{\pi}\right)^{1/3}n(r)^{1/3} \text{ ---- (2.53)}$$

$$n=\left(\frac{4\pi}{3}r_{s}^{3}\right)^{-1} \text{ ---- (2.54)}$$

In LDA, the exchange of uniform electron gas of a density equal to the density at the point where the exchange is to be assessed is used:

$$E_{xc}^{LDA}[n]=-\frac{3}{4\pi}\left(3\pi^{2}\right)^{1/3}\int n^{4/3}(r)d^{3}r \text{ ---- (2.55)}$$

However, a serious limitation of LDA is that it cannot provide estimation to the long-ranged van der Waals (vdW) interaction[18].

2.4.2. Generalized gradient approximation (GGA)

The generalized gradient approximation (GGA) improves upon the LDA by incorporating first-order gradient terms, making the exchange-correlation energy dependent on both the local densities and their gradients 1[12,13]. The functionals are generally defined as:

$$E_{xc}^{GGA}[n^{\uparrow},n^{\downarrow}]=\int n(r)\varepsilon_{xc}\left(n^{\uparrow},n^{\downarrow},\left|\nabla n^{\uparrow}\right|,\left|\nabla n^{\downarrow}\right|\right)d^{3}r \text{ ---- } (2.56)$$

$$E_{xc}^{GGA}[n^{\uparrow},n^{\downarrow}]=\int n(r)\varepsilon_{x}^{\text{hom}}(n)F_{xc}\left(n^{\uparrow},n^{\downarrow},\left|\nabla n^{\uparrow}\right|,\left|\nabla n^{\downarrow}\right|\right)d^{3}r \text{ ---- } (2.57)$$

Where F_{xc} represents dimensionless quantities and $\varepsilon_{x}^{\text{hom}}(n)$ is the exchange energy. The GGA is popular due to its moderate computational cost and simplicity. Among the many functionals, the most widely used are those proposed by Becke, Perdew and Wang (PW)[19], and Perdew, Burke, and Enzerhof (PBE)[20]. Numerous studies have shown that the GGA reduces the LDA errors in calculating cohesive energies of solids and molecules and provides more accurate equilibrium lattice parameters compared to the LDA[21].

2.4.3. Pseudopotentials

In many instances, it is practical to simplify Density Functional Theory (DFT) calculations by explicitly describing only the valence electrons, achieved through the use of 'pseudopotentials'. These computational tools facilitate the treatment of core and valence electrons distinctly: core electrons, tightly bound to the nucleus, remain 'frozen' in their isolated atomic state, while valence electrons, more loosely bound and localized further from the nucleus, are actively involved in chemical interactions. When differentiating between core and valence states in polyatomic systems, this approach allows for efficient computational modeling. Core electrons, maintained in their isolated atomic configuration, obviate the need for detailed Kohn–Sham wave functions, leading to significant computational savings. However, accurately defining valence states involves careful adjustment near the nucleus to ensure proper orthogonality to core states, crucial for maintaining correct 'nodal structures' in valence wave functions.

Challenges arise in accurately describing these oscillatory features within real-space grids or plane wave bases, which can impact computational accuracy and stability. Finer grid resolutions or higher kinetic energy cut-offs may mitigate these issues but at the cost of increased computation time. Alternatively, employing pseudowave functions that smooth out nodal complexities within the pseudization region resolves these challenges. This method involves adjusting the nuclear potential in such a way that it preserves the integrity of the

Kohn–Sham equations, ensuring accurate representation of electronic behaviors. Pseudopotentials, particularly Ultrasoft types, play a pivotal role in this process. They transform the computational framework by introducing auxiliary functions around each ion core, facilitating precise calculations while maintaining computational efficiency. These pseudopotentials are designed to meet stringent requirements for accurate ab-initio simulations, as outlined by Hamann, Schlüter, and Chiang[22].

Integrating with the Perdew-Burke-Ernzerhof (PBE) exchange-correlation functional further enhances the accuracy and versatility of DFT calculations. PBE, within the generalized gradient approximation (GGA), improves upon earlier methods by providing a more refined description of exchange and correlation energies between electrons[20]. Widely utilized in materials science and quantum chemistry, PBE accurately predicts properties such as bond lengths, lattice constants, and electronic structures of diverse materials. In summary, combining pseudopotential methodologies like Ultrasoft with the PBE functional not only simplifies the treatment of core and valence electrons but also enhances the precision and efficiency of predictive modelling in DFT. This integrated approach balances theoretical rigor with computational feasibility, advancing our ability to understand and manipulate material properties at the atomic scale effectively.

2.5. Boltzmann Transport Equation and BoltzTraP

The Boltzmann Transport Equation (BTE) is a fundamental equation in solid-state physics used to describe the transport of charge carriers (electrons or holes) through a crystalline material. It relates the distribution function of carriers to their scattering processes, providing a theoretical framework for calculating electrical conductivity, thermal conductivity, and other transport properties based on the material's electronic band structure and scattering mechanisms. The BTE in its general form is expressed as[23]:

$$\frac{\partial f(\boldsymbol{k},\boldsymbol{r},t)}{\partial t} + \boldsymbol{v}(\boldsymbol{k}) \cdot \boldsymbol{\nabla}_{\boldsymbol{r}} f(\boldsymbol{k},\boldsymbol{r},t) + \boldsymbol{F}(\boldsymbol{k}) \cdot \boldsymbol{\nabla}_{\boldsymbol{r}} f(\boldsymbol{k},\boldsymbol{r},t) = \left(\frac{\partial f(\boldsymbol{k},\boldsymbol{r},t)}{\partial t}\right)_{coll} \text{ ---- } (2.58)$$

Where, $f(\boldsymbol{k},\boldsymbol{r},t)$ is the distribution function of carriers (electrons or holes) depending on wave vector, position, and time. $\boldsymbol{v}(\boldsymbol{k})$is the velocity of the carriers at wave vector. $\boldsymbol{F}(\boldsymbol{k})$ represents external forces acting on the carriers, such as electric and magnetic fields. $\left(\frac{\partial f(\boldsymbol{k},\boldsymbol{r},t)}{\partial t}\right)_{coll}$ denotes the collision integral, describing the rate at which carriers scatter due to interactions with the crystal lattice, impurities, or other carriers.

The BTE forms the foundation of BoltzTraP, a versatile tool for computing electronic band structures and deriving material properties based on theoretical principles[24]. Leveraging methodological advancements, user-friendly distributed codes, and increased computational power, BoltzTraP simplifies the calculation of complex band structures. Central to the approach of BoltzTraP is a Fourier expansion of band energies, preserving space group symmetry through star functions. This technique ensures that extrapolated energies precisely match computed band energies, minimizing discrepancies using a roughness function to suppress oscillations between data points.

This analytical framework enables straightforward computation of band-dependent quantities critical for understanding material behavior. The reliability of BoltzTraP has been validated across diverse applications, from intermetallic compounds to high-temperature superconductors and thermoelectric materials. It consistently demonstrates excellent agreement with experimental data, including challenging properties like the Hall coefficient, which relies on precise second derivatives of band structures. Despite Boltzmann theory's inherent limitations, particularly concerning band crossings affecting derivative calculations, BoltzTraP remains indispensable. It offers a well-documented, reliable platform for theoretical exploration and prediction of material properties, empowering researchers in materials science to gain accurate insights from electronic band structures and transport coefficients[25].

2.5.1. Electrical Conductivity Calculation

BoltzTraP calculates electrical conductivity by leveraging a Fourier expansion of the band energies while maintaining the space group symmetry using star functions[26].

$$\widetilde{\in}_{\iota}\,(\boldsymbol{k}) = \sum_R c_{Ri} S_R(\boldsymbol{k}) \text{ ---- (2.59)}$$

Where, R is a direct lattice vector. $S_R(\boldsymbol{k})$ is called the Star function. Given by:

$$S_R(\boldsymbol{k}) = \frac{1}{n}\sum_{\{\Lambda\}} e^{1\boldsymbol{k}\cdot\Lambda\mathbf{R}} \text{ ---- (2.60)}$$

With the Fourier-expanded band energies, the electrical conductivity tensor, can be calculated as described:

$$\sigma_{\alpha\beta}(\mu, T) = \frac{1}{N}\sum_k \tau(\boldsymbol{k}) v_\alpha(\boldsymbol{k}) v_\beta(\boldsymbol{k}) \left[-\frac{\partial f_0(\in(\boldsymbol{k}),\mu,T)}{\partial k}\right] \text{ ---- (2.61)}$$

i. **Group Velocity Calculation:** The group velocity $v_\alpha(\boldsymbol{k})$ is obtained from the electronic band structure, specifically from the derivative of the energy with respect to the wave vector:

$$v_\alpha(\boldsymbol{k}) = \frac{1}{\hbar}\frac{\partial \in(\boldsymbol{k})}{\partial k_\alpha} \text{ ---- } (2.62)$$

ii. **Fermi-Dirac Distribution Function**: The Fermi-Dirac distribution function and its derivative with respect to energy are given by:

$$f_0(\in, \mu, T) = \frac{1}{\exp\left(\frac{\in-\mu}{k_B T}\right)+1} \text{ ---- } (2.63)$$

iii. **Relaxation Time Approximation**: In BoltzTraP, the relaxation time is often assumed to be constant for simplicity, which allows separating the intrinsic material properties from the scattering processes. The electrical conductivity then becomes:

$$\sigma_{\alpha\beta}(\mu, T) = \tau \cdot \sum\nolimits_{\alpha\beta}(\mu, T) \text{ ---- } (2.64)$$

Where, $\sum_{\alpha\beta}(\mu, T)$ is the transport distribution function. Which is essential for calculating transport properties such as electrical conductivity. It represents the probability distribution of charge carriers (electrons or holes) in momentum space, considering their energy states and velocities under the influence of external fields and scattering mechanisms[27].

2.5.2. Steps for BoltzTraP

By following the steps below, BoltzTraP can provide insights into the transport properties of materials, including the electrical conductivity, based on the underlying electronic structure obtained from DFT calculations[24].

Step 1 (Electronic Structure Calculation): Perform a DFT calculation to obtain the electronic band structure and eigenvalues for each band and wave vector.

Step 2 (Interpolation): Use the Fourier interpolation method provided by BoltzTraP to interpolate the band structure onto a dense k-point mesh.

Step 3 (Velocity Calculation): Calculate the group velocities from the interpolated band structure.

Step 4 (Transport Distribution Function): Compute the transport distribution function using the velocities and the derivative of the Fermi-Dirac distribution.

Step 5 (Electrical Conductivity): Calculate the electrical conductivity using the transport distribution function and an assumed or calculated relaxation time.

BIBLIOGRAPHY:

1 P. Giannozzi, S. Baroni, N. Bonini, M. Calandra, R. Car, C. Cavazzoni, D. Ceresoli, G. L. Chiarotti, M. Cococcioni, I. Dabo, A. Dal Corso, S. De Gironcoli, S. Fabris, G. Fratesi, R. Gebauer, U. Gerstmann, C. Gougoussis, A. Kokalj, M. Lazzeri, L. Martin-Samos, N. Marzari, F. Mauri, R. Mazzarello, S. Paolini, A. Pasquarello, L. Paulatto, C. Sbraccia, S. Scandolo, G. Sclauzero, A. P. Seitsonen, A. Smogunov, P. Umari and R. M. Wentzcovitch, *J. Phys. Condens. Matter*, 2009, **21**, 44.

2 E. Schrödinger, *Phys. Rev.*, 1926, **28**, 1049–1070.

3 M. Born and R. Oppenheimer, *Ann. Phys.*, 1927, **389**, 457–484.

4 C. A. Coulson, *Rev. Mod. Phys.*, 1960, **32**, 170–177.

5 F. Giustino and R. Books, 2014, 11–12.

6 D. R. Hartree and W. Hartree, *Proc. R. Soc. London. Ser. A - Math. Phys. Sci.*, 1935, **150**, 9–33.

7 J. C. Slater, 1951.

8 L. H. Thomas, *Math. Proc. Cambridge Philos. Soc.*, 1927, **23**, 542–548.

9 E. Fermi, *Zeitschrift Fur Phys.*, 1928, **48**, 73–79.

10 C. F. v. Weizsäcker, *Zeitschrift für Phys.*, 1935, **96**, 431–458.

11 E. Runge and E. K. U. Gross, *Phys. Rev. Lett.*, 1984, **52**, 997–1000.

12 W. Kohn, A. D. Becke and R. G. Parr, *J. Phys. Chem.*, 1996, **100**, 12974–12980.

13 A. D. Becke, *J. Chem. Phys.*, 1993, **98**, 1372–1377.

14 H. Raza, *Nanosci. Technol.*, 2019, 29–76.

15 B. A. Wells and A. L. Chaffee, *J. Chem. Theory Comput.*, 2015, **11**, 3684–3695.

16 R. Nityananda, P. Hohenberg and W. Kohn, *Resonance*, 2017, **22**, 809–811.

17 J. W. Negele, *Phys. Rev. C*, 1970, **1**, 1260–1321.

18 T. Jenkins, K. Berland and T. Thonhauser, 2021, 3–7.

19 K. Burke, J. P. Perdew and Y. Wang, *Electron. Density Funct. Theory*, 1998, 81–111.

20 J. P. Perdew and K. Burke, *Phys. Rev. B - Condens. Matter Mater. Phys.*, 1996, **54**, 16533–16539.

21 P. M. W. Gill, B. G. Johnson, J. A. Pople and M. J. Frisch, *Chem. Phys. Lett.*, 1992, **197**, 499–505.

22 D. R. Hamann, M. Schlüter and C. Chiang, 1979, **1494**, 1–7.

23 X. He and L. S. Luo, *Phys. Rev. E - Stat. Physics, Plasmas, Fluids, Relat. Interdiscip. Top.*, 1997, **55**, 6811–6820.

24 G. K. H. Madsen and D. J. Singh, *Comput. Phys. Commun.*, 2006, **175**, 67–71.

25 R. N. Euwema, D. J. Stukel, T. C. Collins, J. S. Dewitt and D. G. Shankland, *Phys. Rev.*, 1969, **178**, 1419–1423.

26 A. Faghaninia, J. W. Ager and C. S. Lo, *Phys. Rev. B - Condens. Matter Mater. Phys.*, 2015, **91**, 1–14.

27 D. D. Koelling and J. H. Wood, *J. Comput. Phys.*, 1986, **67**, 253–262.